Available online at www.sciencedirect.com
ScienceDirect
Advances in Space Research 41 (2008) 1882–1893
ADVANCES IN SPACE RESEARCH (a COSPAR publication)
www.elsevier.com/locate/asr

Remote sensing of aerosol and radiation from geostationary satellites

Istvan Laszlo [a,*], Pubu Ciren [b], Hongqing Liu [b], Shobha Kondragunta [a], J. Dan Tarpley [a], Mitchell D. Goldberg [a]

[a] National Oceanic and Atmospheric Administration, 5200 Auth Rd., Camp Springs, MD 20746, USA
[b] QSS Group Inc., 4500 Forbes Boulevard, Lanham, MD 20706, USA

Received 8 November 2006; received in revised form 8 May 2007; accepted 26 June 2007

Abstract

The paper presents a high-level overview of current and future remote sensing of aerosol and shortwave radiation budget carried out at the US National Oceanic and Atmospheric Administration (NOAA) from the US Geostationary Operational Environmental Satellite (GOES) series. The retrievals from the current GOES imagers are based on physical principles. Aerosol and radiation are estimated in separate processing from the comparison of satellite-observed reflectances derived from a single visible channel with those calculated from detailed radiative transfer. The radiative transfer calculation accounts for multiple scattering by molecules, aerosol and cloud and absorption by the major atmospheric gases. The retrievals are performed operationally every 30 min for aerosol and every hour for radiation for pixel sizes of 4-km (aerosol) and 15- to 50-km (radiation). Both retrievals estimate the surface reflectance as a byproduct from the time composite of clear visible reflectances assuming fixed values of the aerosol optical depth. With the launch of GOES-R NOAA will begin a new era of geostationary remote sensing. The Advanced Baseline Imager (ABI) onboard GOES-R will offer capabilities for aerosol remote sensing similar to those currently provided by the Moderate Resolution Imaging Spectroradiometer (MODIS) flown on the NASA Earth Observing System (EOS) satellites. The ABI aerosol algorithm currently under development uses a multi-channel approach to estimate the aerosol optical depth and aerosol model simultaneously, both over water and land. Its design is strongly inspired by the MODIS aerosol algorithm. The ABI shortwave radiation budget algorithm is based on the successful GOES Surface and Insolation Product system of NOAA and the NASA Clouds and the Earth's Radiant Energy System (CERES), Surface and Atmospheric Radiation Budget (SARB) algorithm. In all phases of the development, the algorithms are tested with proxy data generated from existing satellite observations and forward simulations. Final assessment of the performance will be made after the launch of GOES-R scheduled in 2012.
Published by Elsevier Ltd on behalf of COSPAR.

Keywords: Aerosol; Shortwave radiation budget; Geostationary satellite

1. Introduction

Aerosols are ever-present and highly-varying constituents of our atmosphere. They play roles in many physical and chemical processes that shape the composition of the atmosphere and thereby affect cloud formation, visibility, and air quality. They interact both directly and indirectly with radiation and thus affect the amount of radiative energy reaching the surface and reflected to space. The shortwave part of the radiative energy at the surface (insolation) is an important component of the surface energy budget, and a necessary input to models of land-surface processes.

Real time monitoring of aerosol and surface insolation from Geostationary Operational Environmental Satellite (GOES) data have been routinely conducted at the US National Oceanic and Atmospheric Administration (NOAA), National Environmental Satellite, Data and Information Service (NESDIS). The advantage of doing this from a geostationary platform is obvious for solar radiation budget, and that is the ability of resolving the diurnal cycle needed for an accurate estimate of the daily

* Corresponding author. Tel.: +1 301 763 8053.
E-mail address: istvan.laszlo@noaa.gov (I. Laszlo).

0273-1177/$34.00 Published by Elsevier Ltd on behalf of COSPAR.
doi:10.1016/j.asr.2007.06.047

total insolation. Frequent observations of the same area available only from geostationary orbits are also important for air quality monitoring since they permit tracking the rapid movement of pollution.

Retrievals of aerosol optical depth and shortwave radiation budget from geostationary satellite measurements already have a long history; here only a few representative works will be cited. Many of these works take advantage of the nearly constant view geometry and/or the high temporal resolution provided by geostationary satellites. For example, Fraser et al. (1984) estimated aerosol optical depth (AOD) from the GOES imager over the eastern US using the difference in optical thickness between subsequent scenes and the fact that over dark surfaces (albedo <0.15 in the visible) the reflection increases as the optical depth increases. Knapp (2002) and Knapp et al. (2002) estimated the surface albedo from a series of consecutive GOES-8 images and retrieved the AOD for the US and over South America. Zhang et al. (2001) and Christopher et al. (2002) used a similar method to estimate the surface albedo and retrieved the AOD from high temporal resolution GOES-8 imager radiances and detailed radiative transfer calculations. Pinty et al. (2000a,b) exploited the frequent (every 30 min) Meteosat observations to estimate the surface albedo and the aerosol optical depth (held constant throughout the day) simultaneously.

Observations of geostationary satellites are also used for characterizing the solar (shortwave) energy balance of our planet and the solar irradiance reaching the surface. Using a statistical method, Tarpley (1979) demonstrated that insolation can be determined from the Visible and Infrared Spin Scan Radiometer (VISSR) on GOES. Gautier et al. (1980) developed a physical model that accounted for molecular scattering and cloud extinction, and applied it to estimate insolation from GOES radiances. Pinker and Laszlo (1992) designed another physical method that in addition to gas absorption accounted for both aerosol and cloud extinction. Regional and global applicability of their model was demonstrated with GOES-5 VISSR data and with geostationary radiances from the International Satellite Cloud Climatology Project (ISCCP, Schiffer and Rossow, 1983) B3 data. The same algorithm was adopted by NOAA/NESDIS in the GOES Surface and Insolation Product (GSIP, Pinker et al., 2002). GOES data and models for estimating the radiation budget are also used for quantifying the effects of the various components of the atmosphere-surface system have on the energy balance. For example, Harrison and Minnis (1983) used GOES imager data to estimate the influence of clouds on the radiation budget. Futyan et al. (2005) employed high temporal resolution Meteosat 8 data to estimate the contribution of individual cloud types to cloud forcing. GOES-derived insolation data are also used in land data assimilation projects (Pinker et al., 2003). Because of the characteristics of the satellite instruments used in the studies mentioned above, the shortwave (SW) radiation budget is estimated from the narrowband measurements of the imagers. The first instrument dedicated to the direct measurement of the shortwave and longwave radiation budget from geostationary orbit is the Geostationary Earth Radiation Budget (GERB) instrument onboard the Meteosat-8 spacecraft operated by the European Organization for Exploitation of Meteorological Satellites (EUMETSAT) (Harries et al., 2005). Currently there is no plan to have a similar instrument on the US GOES series of satellites, so the radiation budget must continue to be derived from the narrowband radiance measurements.

The potential for retrieving aerosol and radiation budget will be substantially improved with the new Advanced Baseline Imager (ABI) scheduled to fly on the GOES-R satellite around 2012. ABI will have many more channels, higher spatial resolution, and faster imaging than the current GOES imager has. Image navigation, registration, and radiometric performance will also be improved, and ABI is expected to have on-board calibration of the visible channels (Schmit et al., 2005). Because of the similarity of its spectral channels to those of the Moderate Resolution Imaging Spectroradiometer (MODIS; King et al., 1992) flown on the NASA Earth Observing System (EOS) satellites, ABI will offer capabilities for aerosol remote sensing similar to those currently provided by MODIS. It is expected that ABI will also present a better estimate of the shortwave radiation budget. The increase in the number of channels should lead to a more accurate top of atmosphere reflected flux. By providing an improved constrain at the top, and more accurate aerosol and cloud information, the retrieval of the shortwave downward flux at the surface should also become more accurate.

The Center for Satellite Applications and Research (STAR) at NOAA/NESDIS is currently engaged in the development of algorithms for the retrieval of a suite of geophysical parameters from ABI on GOES-R. The current paper gives a high-level overview of these activities as they related to the remote sensing of aerosol and radiation budget. In the next sections, the main features of the ABI and those of the current imager are briefly compared, aerosol and insolation retrievals from the current GOES are summarized, and the ABI-based retrieval techniques currently under development at STAR for aerosol and radiation budget are described.

2. ABI and the current imager

The imager on the current GOES (GOES 12) has one band in the visible (0.65 μm) and four bands (3.9, 6.5, 10.7, and 13.3 μm) in the infrared; it has no near-infrared channels. The nominal subsatellite instantaneous geometric field of view (IGFOV) is 1 km for the visible channel, and 4 km for the infrared channels, except for the 13.3-μm band that has an IGFOV of 8 km. Remote sensing of most geophysical parameters, particularly the retrieval of aerosol optical depth, requires accurate measurements of radiances. However, the visible channel is not calibrated onboard, and this makes aerosol retrieval challenging. To

alleviate this shortcoming, various vicarious calibration methods are applied, which include monitoring of targets with known reflectance, assumed to be stable in time (e.g. Knapp and Vonder Haar, 2000) and by comparing GOES radiances to calibrated radiances from other satellites, like MODIS (XiangqianWu, personal communication). In contrast to the current imager, ABI will have 16 spectral channels; six of these are in the shortwave spectrum (0.47, 0.64, 0.865, 1.378, 1.61, and 2.25 μm), and the rest (3.9, 6.19, 6.95, 7.34, 8.5, 9.61, 10.35, 11.2, 12.3, and 13.3 μm) are in the infrared. The nominal IGFOV of the infrared and of the 2.25 and 3.9-μm channels is 2 km; that in the shortwave is 1 km with the exception of the 0.64-μm channel, which has an IGFOV of 0.5 km. The main characteristics of the ABI and those of the current imager are summarized in Table 1, where the spectral and spatial coverage, spatial resolution, and availability of onboard calibration are indicated. Fig. 1 shows the simulated spectral response functions of the ABI shortwave channels (ftp://ftp.ssec.wisc.edu/ABI/SRF). For comparison, the spectral response function of the current imager, which is significantly wider than that of any of the ABI channels, is also displayed. Detailed information on the ABI and its comparison with the current imager is given by Schmit et al. (2005).

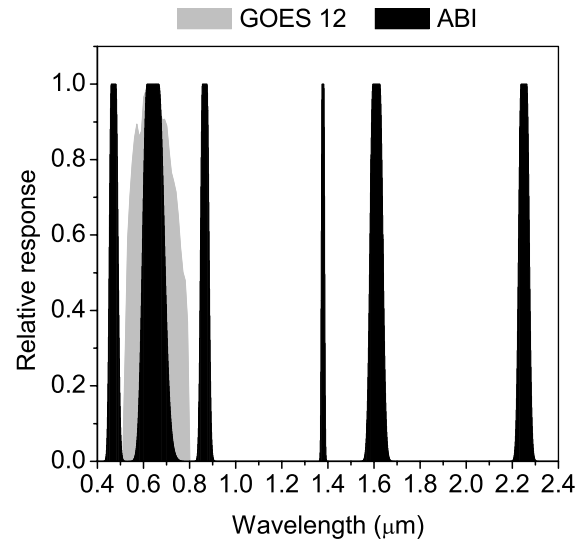

Fig. 1. Simulated relative spectral response functions of the shortwave channels of the Advanced Baseline Imager (ABI). The response function of the visible channel of the imager on the current GOES 12 satellite is also shown for comparison.

3. Aerosol retrieval

3.1. Aerosol retrieval for the current GOES satellites

Aerosol optical depth has been routinely retrieved at NESDIS/STAR for the contiguous US (CONUS) from the GOES-East satellite located over the equator at 75° W. The product is known as the GOES Aerosol and Smoke Product (GASP). It includes retrievals for nominal 4-km pixels every 30 min approximately between 12 UTC and 21 UTC at 15 and 45 min after the hour during daytime. The technique has been described in detail by Knapp (2002) and by Knapp et al. (2002); only the main features of the algorithm are highlighted here.

The methodology assumes that reflective properties of the surface remain unchanged over a sufficiently long period of time (14–28 days), and aerosol increases the cloud-free reflectance at the top of the atmosphere. The consequence of the latter assumption is that retrievals are not performed for bright surfaces. AOD is derived for the effective wavelength of 550 nm from cloud-free radiances in the GOES imager visible band (0.52–0.72 μm). Cloud-free scenes are identified using a cloud mask based on spatial and spectral tests similar to those developed for AVHRR (Pavolonis et al., 2005). The retrieval process starts out with establishing a composite clear scene from which the surface albedo is estimated. The composite is created by selecting the second darkest pixel from the visible images of the most recent 14–28 days. The reason for selecting the second darkest pixel instead of the darkest one is to minimize the effect of cloud shadows that tend to make the clear composite field darker than it should be. The composite is updated every time the retrieval runs. Next, the surface albedo is retrieved from the composite reflectance assuming a minimum aerosol optical thickness of 0.02 at 550 nm. Once the surface albedo is known, AOD is retrieved by comparing the instantaneous satellite-observed reflectance with calculated top-of-atmosphere reflectances.

To eliminate residual cloud contamination, the standard deviation of AOD in a 3×3 box surrounding the target pixel is calculated, and the AOD is discarded if it is larger than a threshold value. Valid AOD retrievals also require the target clear pixels to be at least five pixels away from cloud edges. In the surface albedo and AOD retrievals a look-up table (LUT) is used for efficiency. The LUT is calculated with the Second Simulation of the Satellite Signal in the Solar Spectrum (6S) radiative transfer model (Vermote et al., 1997) assuming a Lambertian surface. The current LUT is based on a single (continental) aerosol model, and thus it does not account for the variability in chemical composition and size distribution. Other shortcomings of

Table 1
Main characteristics of the imager on the current GOES and those of the ABI

		Current imager	ABI
Number of bands		5	16
Spatial resolution	0.64-μm band	~1 km	0.5 km
	Other VIS/NIR bands	n/a	1 km
	Bands >2 μm	~4 km	2 km
Spatial coverage	Full disk	Every 3 h	4/h
	CONUS	~4/h	12/h
	Mesoscale	n/a	Every 30 s
Onboard VIS calibration		No	Yes

the current algorithm include the already mentioned fixed minimum AOD, and fixed gas absorption.

The availability of only a single channel and the lack of on-orbit calibration severely limit the quality of aerosol retrievals from the current GOES satellites. Nevertheless, comparisons of AOD with ground observations at 36 Aerosol Robotic Network (AERONET, Holben et al., 1998) sites show the retrievals to be within ±0.13 of the AERONET values (Knapp et al., 2005).

3.2. Development of the ABI aerosol retrieval algorithm

The ABI algorithm is designed to closely follow the approach used in the MODIS aerosol retrieval (Kaufman et al., 1997; Tanré et al., 1997; Remer et al., 2005). This is partly because of the similarities of the ABI and MODIS spectral channels used for aerosol retrieval and partly because the MODIS-approach has already been proven and well tested. The algorithm retrieves the aerosol optical depth and the most likely aerosol model simultaneously from radiances observed in the visible and near infrared channels. One of the necessary (and probably the most challenging) steps in any aerosol retrieval is the separation of the aerosol signal from that of the surface. The assumption in the ABI algorithm is that the contribution of the ocean surface can be accurately computed, and the land surface reflectance can be estimated from observations. Therefore there are two separate components of the algorithm; one is for land and the other is for ocean. Over the ocean surface reflectance is modeled accounting for wind speed and direction, and for sun-glint, while land surface reflectances in the visible spectrum is estimated from the reflectance in the near infrared (NIR) using pre-determined relationships between visible and NIR reflectances. Because such relationships are only established for the blue (0.47 μm) and the red (0.64 μm) bands (Kaufman et al., 2002), the aerosol retrieval over land uses the clear radiances only in the 0.47, 0.64, and 2.25-μm bands.

The flowchart of the aerosol retrieval over land is shown in Fig. 2. The procedure starts with the selection of non-water pixels, out of which coastal pixels are assigned a degraded quality flag. The normalized difference vegetation index (NDVI) is used to select dark pixels for which the surface-reflectance relationships are assumed to be valid. Assuming that most aerosols are transparent at 2.25 μm the NIR surface reflectance of these pixels is determined, from which then the surface reflectances in the blue and the red bands are estimated using the pre-established relationships between these channels (f and g in Fig. 2). Taking advantage of the near-constant viewing geometry of

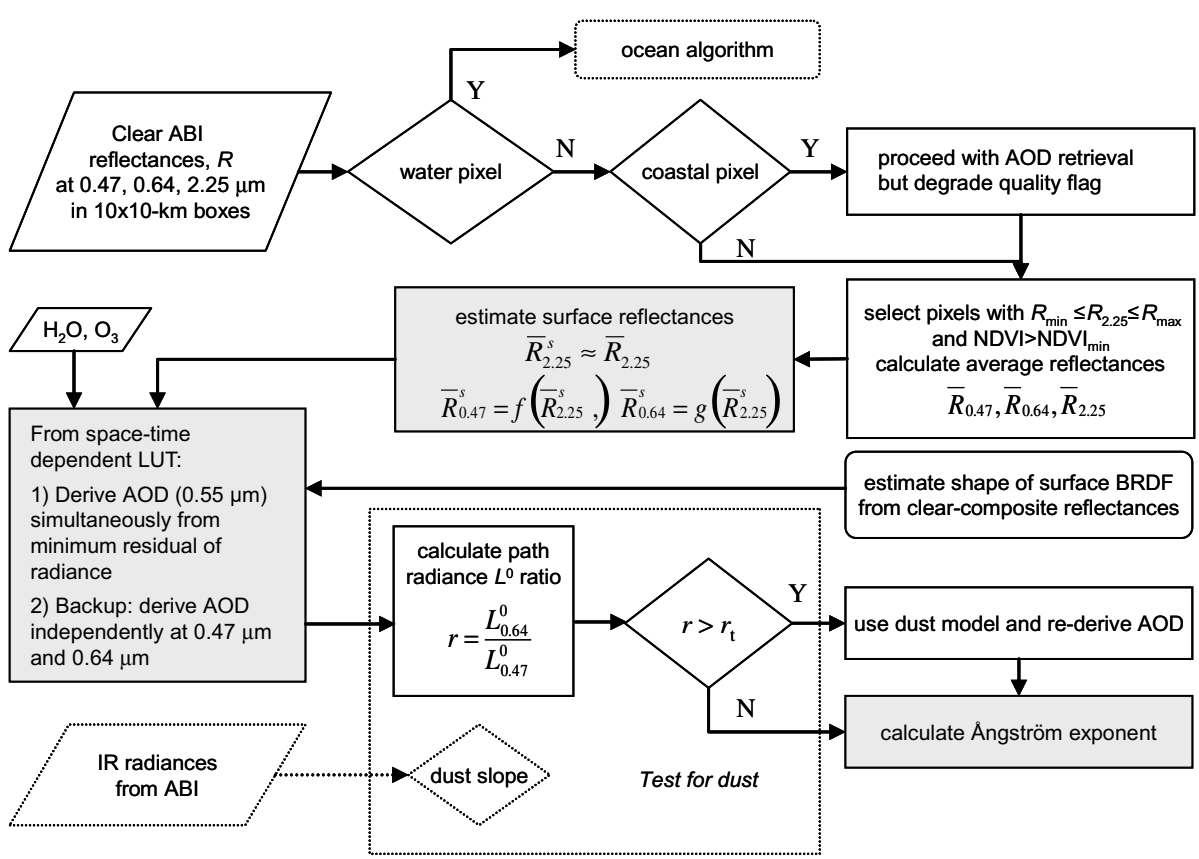

Fig. 2. Flowchart of the planned ABI aerosol retrieval over land. Notation: AOD is aerosol optical depth, Y is yes, N is no, the bar over R means average, the numbers in subscripts denote the wavelength, the superscript "s" means surface, and r_t is the threshold value of the path radiance ratio. See text in Section 3.2 for further details.

geostationary platforms, the surface reflectance retrievals can be further constrained by requiring that they fit a diurnal model of the reflectance. This diurnal model is deduced from a composite of clear reflectances. Knowing the surface reflectances, the top of atmosphere (TOA) blue and red band reflectances are calculated for a set of aerosol optical depths and aerosol models taking the effect of Rayleigh scattering and gas absorption into account. The aerosol properties (AOD and model) are retrieved by comparing the calculated and observed reflectances (see below). Dust is identified from their effect on the IR radiances and by calculating the ratio of the red-to-blue aerosol path radiances (L° in Fig. 2). Since dust absorbs more in the blue band, the ratio is greater than that for a non-dust scene, in which case the previously selected aerosol model is replaced by the dust model and a new AOD is retrieved.

The reflectances due to aerosol for different aerosol amounts and aerosol models are currently calculated with the 6S radiative transfer model (Vermote et al., 1997). The results of the calculations are stored in a look-up table (LUT). Currently, two sets of aerosol models are considered in the LUT. One has eight models that include continental, maritime, dust, oceanic, smoke, and urban models with high and low absorption. The second set is adopted from the Multi-angle Imaging SpectroRadiometer (MISR) project "most likely" climatology. The latter is based on the classification of aggregated results from global transport models. It has 13 types of aerosol mixing groups; each one is based on the relative abundance of four basic components (Kahn et al., 2001). The final climatology of aerosol models will be refined later based on sensitivity studies and better knowledge of aerosol climatology.

From all the optical depths and models in the look-up table, the algorithm selects the AOD and the model that best match the multi-channel observations simultaneously. Mathematically, the retrieved AOD and aerosol model are the ones that provide the smallest residual calculated as $\text{Residual} = \sum_{i=1}^{N}\left[R_i^{\text{obs}} - R_i^{\text{cal}}(\tau)\right]^2$, where N is the number of channels used in the retrieval (two for land and four for ocean), τ is the aerosol optical depth at 550 nm, R_i^{obs} and R_i^{cal} are the observed and calculated reflectances in channel i, respectively. This principle is further illustrated in Fig. 3 where the TOA reflectance in the red (0.64 μm) band is plotted as a function of the TOA reflectance in the blue (0.47 μm) band. For simplicity, Fig. 3 plots the reflectances from the LUT for two aerosol models (models 1 and 2) only. The numbers shown along the curves represent the aerosol optical depth at 0.55 μm. The aerosol optical depth increases from left to right leading to monotonically increasing reflectances. The dotted lines connect reflectances with the same aerosol optical depth. The large diamond in Fig. 3 marks the observed blue and red reflectances, which in this example are 0.2 (blue) and 0.19 (red). Because the reflectance of a snow-free surface is low in the blue band, the blue reflectance is used to retrieve the aerosol optical depth for each aerosol model

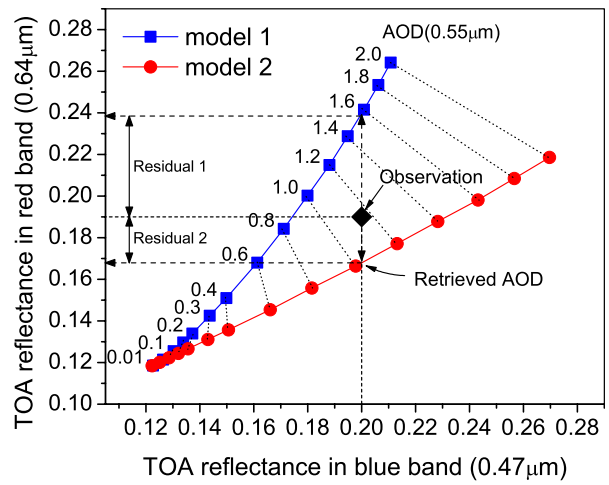

Fig. 3. Illustration of simultaneous retrieval of aerosol optical depth and aerosol model from two channels. The red reflectance is plotted as a function of the blue reflectance for two aerosol models at the discrete values of the optical depth shown along the curve for model 1. The slant dashed lines connect the reflectances corresponding to the same aerosol optical depth. The optical depths retrieved from the blue channel alone are shown by the vertical dashed line. The two red reflectances calculated from the aerosol optical thicknesses retrieved from the blue channel reflectance are shown by the horizontal dashed lines. (For interpretation of the references in color in this figure legend, the reader is referred to the web version of this article.)

in the LUT. In the example shown, the retrieved AOD for model 1 is ~1.6, while that for model 2 is ~1.1. Next, these AOD values are used to calculate the red reflectances for each model leading to the values of ~0.24 and ~0.17 for models 1 and 2, respectively. These red reflectances are then compared to the observed one, and the residuals for each model are calculated. In the example, the residual for model 2 is the smallest and thus the retrieved model is model 2 and the AOD is ~1.1.

Fig. 4a shows a plot of the red and blue reflectances for the eight aerosol models in the current LUT for a selected sun-satellite geometry and atmospheric condition. We note that for low reflectances (small AOD) the separation between some aerosol models is small which can make the AOD and model retrieval ambiguous. This is further illustrated in Fig. 4b, where the red–blue reflectance relationships for the continental and the high absorbing smoke models for low AOD from Fig. 4a are re-plotted. The two curves are almost identical up to about 0.17 in blue reflectance, leading to very similar values of the red-band residuals. The aerosol optical depth values retrieved, however, can be quite different depending on which model is chosen. For example, for the observation marked by the diamond the AOD can be ~0.67 for the continental or ~0.9 for the high absorbing smoke model.

The retrieval principle over ocean is similar to that over land, except the surface reflectance is calculated from a model (Cox and Munk, 1954) as mentioned above, and the aerosol models in the LUT include the combinations of five coarse mode and four fine mode aerosols. The

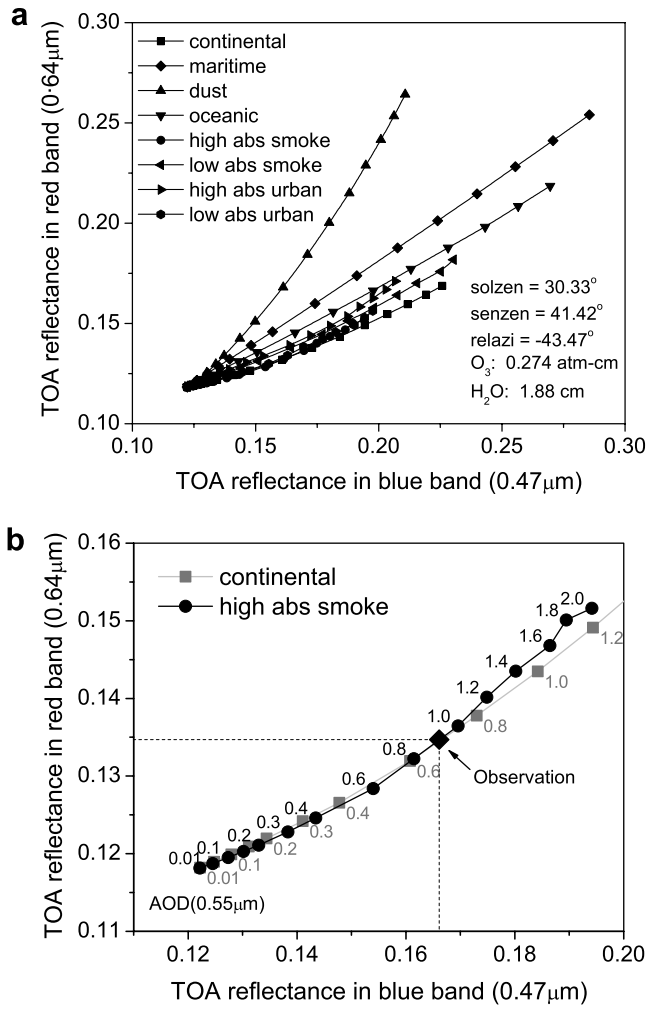

Fig. 4. (a) Red reflectance vs. blue reflectance for the eight aerosol models in the current look-up table for a selected sun-satellite geometry and atmospheric condition. (b) An extract from Fig. 4a showing the red vs. blue reflectance relationships for the continental and the high absorbing smoke models. Note the small separation between the aerosol models for low reflectances. The aerosol optical depth values corresponding to the reflectances for these models are indicated along the curves.

ABI reflectances used are 0.64, 0.86, 1.6, 2.25 μm; the 0.47-μm band is not used over ocean because of the unknown amount of water-leaving radiance at that wavelength.

For algorithm development and testing clear-sky TOA reflectances in the ABI bands are needed. Because the instrument has not yet been built one can only use proxy data for this. One way of getting such data is to use observations from existing satellites. One can use, for example, MODIS reflectances because the spectral placement of the MODIS channels is similar to those of ABI, as shown in Fig. 5 for the shortwave spectrum. The advantage of this approach is that the scenes are realistic. However, some of the MODIS channels do not exactly match the ABI channels so appropriate spectral transformations are needed to convert the MODIS reflectances to ABI reflectances. Such conversions can only be derived from radiative transfer calculations for different (but a limited number of) atmospheric and surface conditions (scenes). These transformations are not expected to

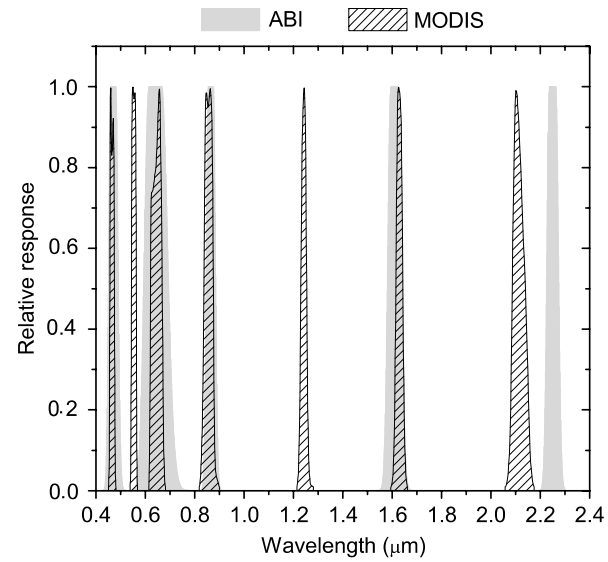

Fig. 5. Relative spectral response functions of the MODIS and ABI shortwave channels used in the aerosol retrieval.

hold for all possible scenes encountered in real observations. One can avoid the spectral conversion if the band-dependent components of the algorithm (e.g. LUT) are built for the MODIS band. In this case, however, one is not actually testing the ABI algorithm.

Another possibility for generating proxy reflectances is to simulate them with a radiative transfer model. The advantage is that one can "match" the ABI channels exactly, and the "true" AOD is also known. However, this approach can only offer a limited realism and because of its nature must be confined to specific, very limited scenes. A third possibility, which has been adopted for the ABI aerosol algorithm development, combines the best of the two approaches mentioned above. In this method, MODIS derived values of atmospheric (cloud mask, AOD, total column ozone, and water vapor) and surface (8-day composite surface reflectance) properties are used with a radiative transfer model. The MODIS products are downloaded from http://ladsweb.nascom.nasa.gov/data/search.html. Because these products are available on different spatial and temporal scales, the ABI "simulator" system first remaps them into a common grid. About 10 "tiles" from the MODIS-derived surface reflectance product are used to cover a single MODIS "granule" from the atmosphere product. The tiles are re-gridded to match the atmosphere-product grid using MODIS re-projection tools. The system then uses the 6S radiative transfer code (Vermote et al., 1997) to calculate the ABI reflectances in the channels used for aerosol retrieval. Fig. 6a shows an example of the ABI reflectance in the blue band simulated from a MODIS granule for April 12, 2003, 18:15 UTC. The AOD (at 550 nm) retrieved is shown in Fig. 6b. In the simulation, the MODIS-derived surface spectral reflectances are assumed to be valid for the ABI bands. In the retrieval of surface reflectance, the MODIS relationships between the blue/red and NIR surface reflectances are used for

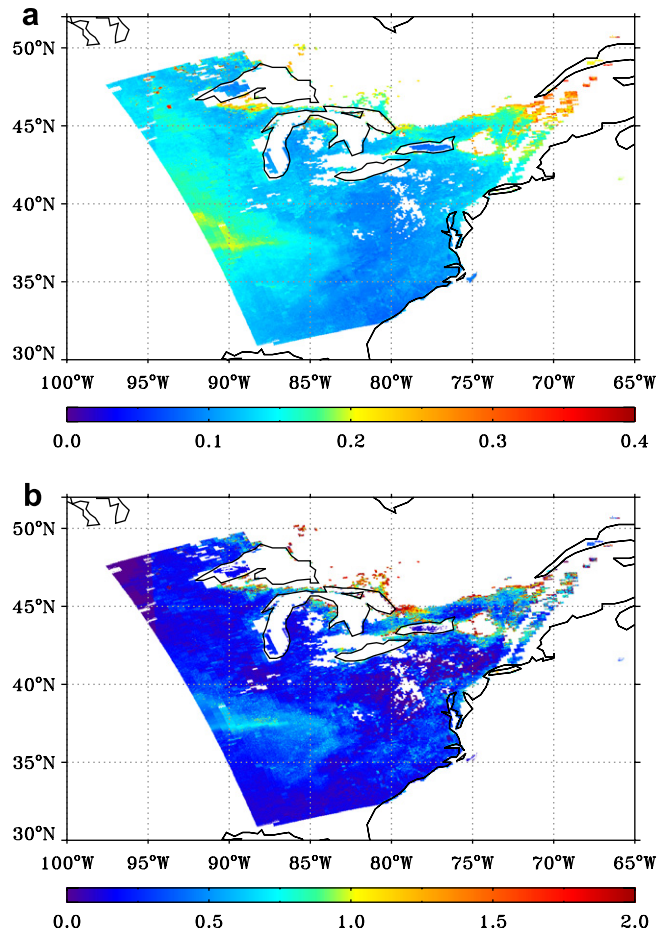

Fig. 6. (a) An example of the ABI reflectance in the blue band simulated from MODIS-derived surface and atmosphere properties for a MODIS granule on April 12, 2003 at 18:15 UTC. (b) The AOD (at 550 nm) retrieved from simulated ABI blue, red and near infrared reflectances. (For interpretation of the references in color in this figure legend, the reader is referred to the web version of this article.)

now since these relationships for ABI has not yet been established. The discontinuity at the upper left corner of the reflectance and AOD fields is an artifact, which will be corrected in future simulations. The elevated AOD values (>1.5) along the edges in the upper right corner are the result of residual snow contamination in the input MODIS AOD field.

4. Shortwave radiation budget retrieval

4.1. Radiation budget from current GOES

The shortwave radiation budget has been retrieved from GOES measurements operationally at NOAA/NESDIS since January 1996. The product is known as the GOES Surface and Insolation Product (GSIP). The GSIP system provides shortwave radiation budget data for the US (CONUS; 24°N–54°N, 66°W–126°W) every daytime hour at a spatial resolution of ~50 km. Images from the GSIP CONUS system can be viewed at http://www.orbit.nesdis.noaa.gov/smcd/emb/gsip/index.htm. The retrieval is based on the work of Pinker and Laszlo (1992); the system as applied to GOES is described in detail in Pinker et al. (2002, 2003). The insolation retrievals over land in GSIP were extensively evaluated by comparing them to values observed at selected sites of the Surface Radiation Monitoring Network (SURFRAD, Augustine et al., 2000). Root mean square (rms) errors were found to be ~90 W m^{-2}, ~25 W m^{-2}, and ~20 W m^{-2} on hourly, daily, and monthly time scales, respectively (Pinker et al., 2003). Another system on a higher spatial resolution (~14 km) is also run experimentally. This high resolution system does retrievals from both the East and the West GOES satellites and also covers larger areas. The radiation budget is estimated for the east (20°S–60°N; 40°W–110°W) and west (0°N–60°N; 100°W–170°W) extended hemispheres every hour; and for the east (60°S–60°N; 15°W–135°W) and west (60°S–60°N; 75°W–165°E) full disks every 3 h. The output includes up- and downwelling shortwave, visible and near infrared direct and diffuse fluxes at the top of the atmosphere and at the surface.

Estimation of the radiation budget is based on the fact that there is a more or less well-defined relationship between the top of atmosphere reflectance and the total downward flux transmittance in the shortwave part of the spectrum. This is because both quantities are determined by the same parameters: aerosol and cloud optical depth, water vapor and ozone absorption, surface albedo and illumination geometry. The relationship between reflectance and transmittance is calculated from a radiative transfer model for discrete values of these parameters and made available in the form of a look up table during the retrieval. The radiative transfer model currently used for this calculation is based on the delta-Eddington approximation and employs parameterizations of ozone and water vapor absorption, and optical properties of aerosol and cloud. Details on the model and its implementation are provided in Pinker and Laszlo (1992) and Laszlo and Pinker (2002).

The transmittance–reflectance relationship and the principle of the radiation budget retrieval are illustrated in Fig. 7 for a clear and a cloudy scene with given values of water vapor and ozone and illumination geometry (solar zenith angle). Fig. 7 plots the shortwave (broadband) flux transmittance as a function of the TOA broadband reflectance for increasing values of the aerosol and cloud optical depths (optical depth increases from left to right). The transmittance–reflectance relationships have different slopes. Because aerosol is more absorbing than cloud in the shortwave, the slope of the relationship for aerosol is steeper. The consequence of this for insolation retrieval is that a given error in the TOA reflectance will have a larger impact on the clear-sky flux retrieval. This is of course just another way of saying that the smaller clear-sky signal is more susceptible for observational errors. The clear and cloudy broadband TOA reflectances, which in the example in Fig. 7 are respectively 0.1 and 0.5, are used to estimate the clear and cloudy transmittances separately from the

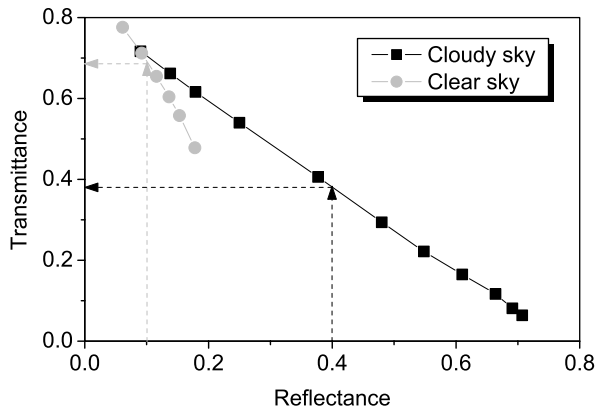

Fig. 7. Illustration of the shortwave transmittance–reflectance relationship and the insolation retrieval process. The TOA shortwave reflectance is estimated from the GOES visible channel. Insolation is calculated from transmittances estimated from the clear and cloudy reflectances as shown.

clear and cloudy relationships as shown by the dashed lines. The transmittances are then multiplied by the TOA downward flux to yield estimates of the clear and cloudy downward fluxes at the surface. The total (all-sky) flux is obtained by calculating an average of these fluxes weighted by the cloud fraction. The TOA downward flux is calculated from the extraterrestrial solar spectrum by accounting for the variation in Sun–Earth distance and the position of the Sun in the sky relative to the local vertical. The upward flux at the surface is obtained by multiplying the downward flux with the surface albedo.

The surface albedo is derived from composite clear TOA broadband albedos created from the darkest pixels of the visible images for the latest 21 days. It is assumed that the clear composite represents cloud-free TOA albedos with known minimum aerosol contributions. The clear composite field is continuously updated to reflect changes caused by seasonal changes in solar illumination and in surface albedo. It also serves as a threshold for cloud detection. The cloud detection employed in the CONUS system is relatively simple; it assumes that any cloud cover in the field of view increases the visible reflectance and its variance. The newer high-resolution algorithm applies additional tests for the presence of clouds. These tests are based on the cloud detection and cloud typing developed for AVHRR (Pavolonis et al., 2005) and include spectral and spatial uniformity tests performed on pixel-level calibrated and geolocated GOES imager radiances in all channels. The pixel-level reflectances are gridded for 0.5-degree (CONUS system) and for 1/8-degree (high-resolution system) targets. For each grid, four classes of data are created: clear, partly clear, partly cloudy, and cloudy. The cloud-typing (Pavolonis et al., 2005) used in the high-resolution system also identifies the dominant cloud type as liquid water, supercooled liquid, thick ice (convective), and thin ice.

The flowcharts presented in Fig. 8 summarize the steps described above. Fig. 8a shows the processes to get the TOA broadband (shortwave) reflectances. The digital

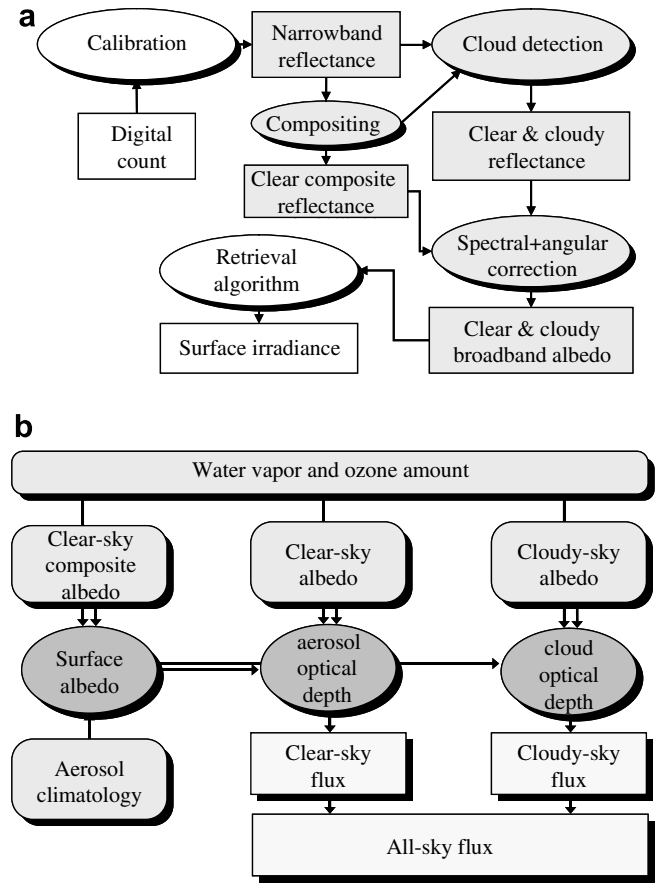

Fig. 8. (a) Flowchart of the processes for deriving clear, cloudy and composite clear broadband albedos. (b) Flowchart of the insolation retrieval from the clear composite, clear and cloudy albedos. See text for details.

counts are converted to narrowband reflectances using the calibration of the visible channel that accounts for the degradation of the sensor (Xiangqian Wu, personal communication). From the narrowband reflectances a composite clear reflectance field is created, and for each target area clear and cloudy reflectances are calculated by averaging the reflectances of clear and cloudy pixels. The latter ones are identified using the compositing and cloud detection procedures mentioned above. The broadband TOA reflectances are estimated from the satellite-observed visible reflectances using spectral and empirical angular conversions. The spectral conversions are derived from linear regression of (narrowband) visible and (broadband) shortwave albedos obtained from radiative transfer simulations performed for a variety of realistic surface and atmospheric conditions. Details on the construction of these conversions are described in Laszlo et al. (1988), Pinker and Laszlo (1992) and Pinker et al. (2003). Fig. 8b displays how the insolation is estimated from the broadband reflectances (albedos). The algorithm takes the amount of water vapor, ozone and snow predicted by forecast systems; all other inputs (composite clear visible reflectance, clear and cloudy reflectance, cloud fraction, cloud type) are derived from observations as mentioned above. After the surface

albedo is estimated from the clear-sky composite reflectance, it is used in the estimation of clear and cloudy fluxes from the clear and cloudy TOA shortwave albedos. These steps essentially retrieve the aerosol and cloud optical depths from the clear and cloudy albedos, respectively.

An example of the instantaneous insolation retrieved in the high-resolution GSIP system from the GOES-12 imager for the full disk is shown in Fig. 9 for August 11, 2004 at 17:45 UTC. At this time the sub-solar point is at about 15° N latitude and 85° W longitude where the surface insolation is at its maximum. Away from this point towards the edges of the image the insolation decreases gradually as the solar zenith angle increases, resulting in a pattern of concentric circles. This simple pattern is modified by the presence of clouds. The image shows Tropical Storms Bonnie in the Gulf of Mexico and Charley in the Caribbean Sea. At the time of the GOES observation (17:45 UTC) Bonnie had maximum sustained winds of 100 km/h, while Charley was nearing hurricane strength and later became a hurricane. Even though both storms were in the vicinity of the sub-solar point at the time of the image was taken the surface insolation dropped below 100 W m^{-2} under these optically thick cloud systems.

Evaluation of the insolation retrievals is done by comparison to values observed at the ground. For this, insolation measurements made at the ground stations of the Surface Radiation Budget Network (SURFRAD, Augustine et al., 2000) are used. An example of a comparison of instantaneous insolation estimated from the high-resolution GSIP system with ground-observed values is shown in Fig. 10 for seven days in July 2004 at Bondville, IL (40.06° N, 88.3° W). The ground data represent three-minute averages of the downward solar flux at the surface. For the comparison, the three-minute-average closest to the time of satellite observation is selected from the ground data. Qualitatively, there is a high degree of agreement between satellite-estimated and ground-measured insolation. This is evident, for example, on July 8 and 10 when changes in insolation caused by changes in cloud amount (fractional cover and/or cloud optical depth) lasting for more than an hour, and recorded by the instrument on the ground are well captured by the GSIP algorithm. This is less successful on days when cloudiness changes more rapidly (July 9 and 11). The scatterplot in Fig. 10 offers a quantitative comparison; the root mean square error (RMSE) of the instantaneous insolation estimate is 146 W m^{-2}, and the

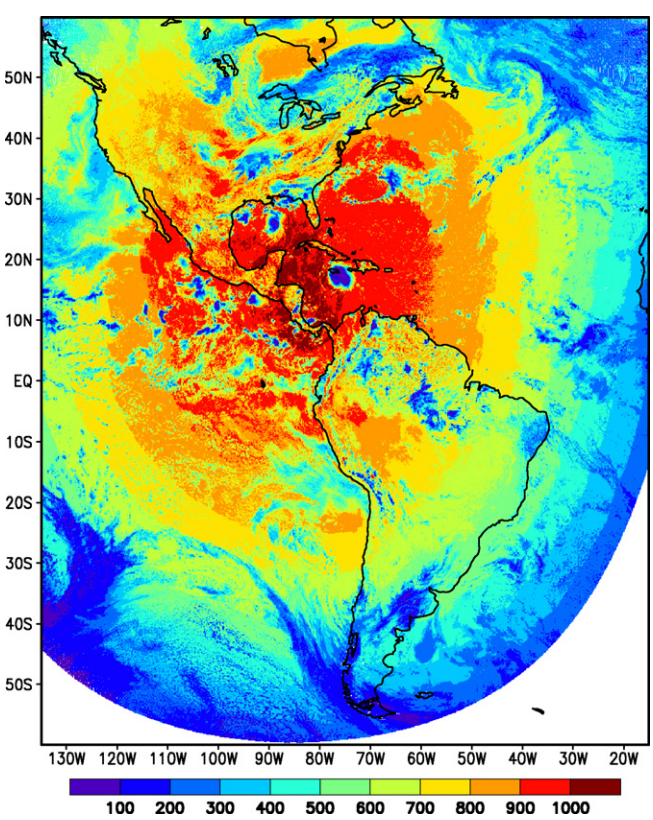

Fig. 9. An example of the full-disk instantaneous insolation retrieved from GOES-12 imager data by the high-resolution GSIP system for August 11, 2004 at 17:45 UTC.

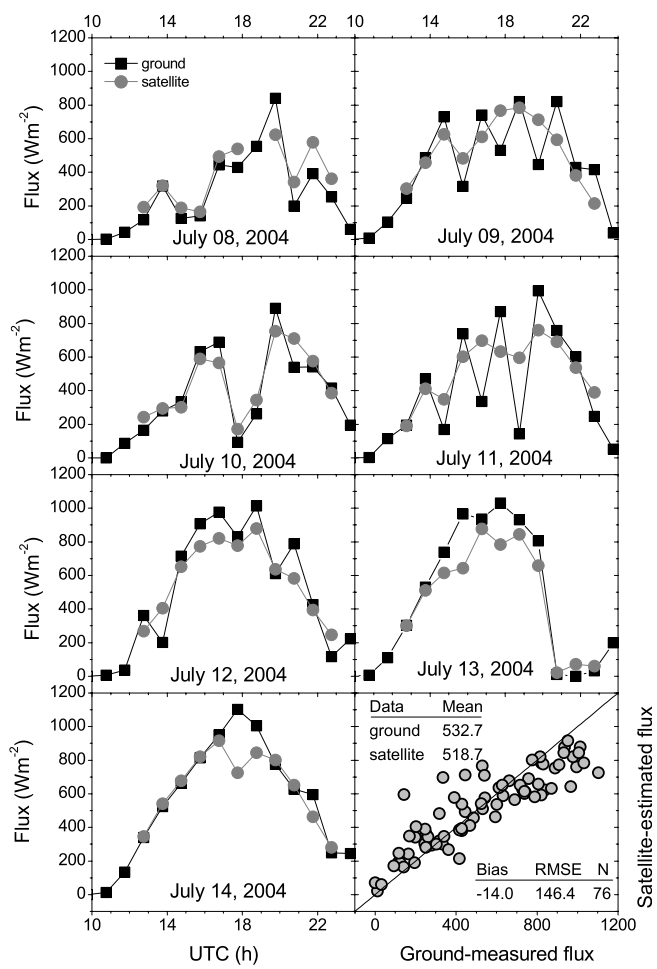

Fig. 10. Comparison of GSIP surface fluxes with those measured at Bondville, IL (40.06° N, 88.3° W) for seven days in July 2004. The ground data represent three-minute averages of the downward solar flux at the surface. For the comparison, the three-minute-average closest to the time of satellite observation was used. Bias is the satellite-ground mean difference, RMSE is the root mean square error, and N is the number of retrievals.

mean of the satellite-estimated insolation for the seven days is 14 W m^{-2} less than that from the ground measurement. The direct comparison of the instantaneous satellite values with three-minute ground averages is simple but not always appropriate. This is because the satellite values represent area averages while the ground measurements correspond to single points. In general, an appropriate temporal average of the ground data is more adequate for comparison with satellite data. Averaging both satellite and ground data for longer time periods (hour, day, and month) also improves the agreement.

4.2. Radiation budget from ABI

The shortwave radiation budget retrieval from ABI is based on the current high-resolution GSIP system, but it takes advantage of the increased spectral information available from ABI. For example, for the estimation of TOA shortwave albedo (and from this the solar energy absorbed by the planet) all six narrowband channels are used instead of the single visible channel available on the current GOES. Bidirectional reflectances and albedos in all six narrowband ABI channels and those in the total shortwave spectrum are computed from a radiative transfer model for a representative selection of realistic scenes. These scenes are simulated from observed atmospheric and surface conditions, similar to those used in the development of the ABI aerosol retrieval. Regression analysis between the narrowband and broadband reflectances and albedos are performed to derive the spectral and angular conversions. These are performed as a function of atmospheric and surface conditions (surface type, cloud amount, phase, optical depth, wind speed) following Loeb et al. (2005). TOA shortwave bidirectional reflectances and albedos obtained by applying the derived spectral and angular conversions are compared to measurements from the Clouds and the Earth's Radiant Energy System (CERES; Wielicki et al., 1996) instrument that measures the TOA shortwave radiation directly, and the conversions are adjusted appropriately. Because radiative transfer simulations can only provide a limited sample of the variety of conditions occurring in nature, the validity of the spectral and angular corrections is expected to be somewhat similarly limited. Therefore, the conversions must be re-derived empirically once actual ABI measurements become available, provided a CERES-type of instrument exists at that time.

The LUT used with the ABI shortwave radiation budget algorithm is updated to account for different cloud phases, more accurate treatment of multiple scattering, and it includes carbon dioxide and oxygen in addition to the currently present water vapor and ozone. Surface albedo retrieval from the clear composite reflectance uses an updated aerosol climatology derived from current satellite (e.g., MODIS) measurements. The ABI channels allow for a more accurate detection of snow, which is one of the largest sources of errors in the current GSIP system.

A whole suite of atmospheric and surface parameters are estimated from the ABI measurements (e.g., water vapor, cloud optical depth, cloud phase, cloud fraction, aerosol optical depth, and surface albedo). These are used in a system similar to the CERES Surface and Atmospheric Radiation Budget (SARB) system (Charlock et al., 2002; Rutan and Charlock, 2004) to obtain an additional estimate of the shortwave radiation budget. CERES/SARB uses observed surface and atmosphere parameters and a radiation transfer model to calculate the shortwave fluxes. This is modified to use look up tables in order to produce the flux estimates in near real time as required. Two separate look up tables are calculated, one for clear and one for cloudy skies (Fred Rose, personal communication). The cloudy table includes inputs of cloud optical depth, cloud particle size, cloud top height and cloud geometric thickness. Two phases of clouds are considered: water and ice. The current clear table has entries for aerosol optical depth and single scattering albedo. Precipitable water, ozone, solar zenith angle, surface altitude, and surface type are inputs to both tables. Surface types include spectrally flat zero and unity albedos, ocean for a fixed chlorophyll and wind speed, cropland, desert, sea ice, and snow. Some of the input parameters needed to estimate the shortwave radiation budget from this system are not going to be available for some locations (for example, aerosol over bright surface), and thus this system does not provide data everywhere. In such cases the missing inputs are supplied from forecast or climatology.

The performance of the two retrievals is systematically tested by analyzing their consistency and by comparing them to ground measurements on different temporal scales. Ideally the two retrievals should lead to identical results. Considering the differences in the approach each retrieval takes for estimating the shortwave radiation budget, this of course is not expected to happen. Moreover, each has its unique advantage over the other. For example, the system based on the current GSIP can potentially provide a more accurate TOA radiation budget since it eventually uses a measurement-based estimation of the broadband albedo. The radiation budget derived by the CERES/SARB-like system, however, is more consistent with the rest of the parameters retrieved from ABI. Optimally, the two systems should run parallel. This would provide independent quality checks and present indispensable diagnostics for monitoring the quality of retrievals. However, external constraints will most likely allow only for a single system. Therefore, after the evaluation one or combination of the two systems will be selected for operational implementation with ABI.

5. Summary

Presently, aerosol optical depth and shortwave radiation budgets are estimated operationally from the visible imager channel of the GOES satellites. The aerosol retrievals are used in air quality studies, verification of model predictions

of pollution (particular matter), planning field campaigns, and aviation, to name a few uses. Those of the radiation budget serve as inputs of radiative forcing in models of land surface processes and coral bleaching.

Retrievals from the ABI instrument on the future GOES-R satellite will serve these needs by providing more accurate estimates and by presenting information that was previously unattainable (e.g., aerosol type) from GOES. The improvements come from the onboard calibration and the use of multiple narrow channels. The latter permits the application of advanced retrieval techniques, such as used, for example, with the MODIS instrument, while the former potentially permits derivation of climate-quality data from the retrievals. As with any multi-channel instrument, monitoring the radiometric performance of the individual channels is critical. Undetected errors in one or a few channels can totally destroy the retrievals. This is especially true for the aerosol retrieval that is usually performed in the low energy regime of the satellite signal (Ignatov, 2003; Ignatov et al., 2005). For this reason and for backup, the ABI aerosol algorithm will also retrieve optical depth in single (individual) channels independently. The final ABI radiation budget algorithm will likely combine the retrieval of fluxes "directly" from observed TOA reflectance (GSIP approach) and that from independently derived surface and atmosphere parameters (CERES/SARB approach). The current GSIP system estimates the TOA shortwave albedo from the relatively broad visible channel. This channel is affected by simultaneous changes of multiple atmospheric and surface parameters. In contrast, the narrower, multiple channels of ABI are "cleaner" in the sense that each channel is sensitive to only a few well defined parameters. This, at least in principle, makes the spectral conversion of narrowband reflectance to broadband shortwave reflectance more accurate (Laszlo et al., 1988).

The algorithms for aerosol and shortwave radiation budget retrieval from ABI are currently under development at NOAA/NESDIS. The development is a collaborative effort of NOAA and the Goddard Earth Science and Technology Center of NASA and the University of Maryland Baltimore County for aerosol and NOAA, NASA Langley Research Center and the University of Maryland at College Park for radiation budget. The development builds upon already existing algorithms as mentioned above. These algorithms have been selected based on their current performance and their potential to fulfill the GOES-R mission requirements (NOAA's Mission Requirements Document 2B Prime (MRD-2B') for the GOES-R Series, Version 2.9, 2006).

Given the close similarity of the instruments and the algorithms, the accuracy of the ABI aerosol algorithm is expected to be similar to that of the MODIS algorithm (Remer et al., 2005). The radiation budget from ABI is likely to be better than that from the current GSIP due to the improvements mentioned above. The algorithms are subjected to extensive testing in all phases of the development. For this, ground observations of the object parameters, existing satellite data (like MODIS) and forward radiative transfer simulations with observed state of the atmosphere and the surface are used to provide proxy ABI radiances. Accuracy of the ABI retrievals is assessed initially using the proxy data. Final assessment of the performance will be performed after the launch of GOES-R.

There is a chance that aerosol and radiation budget retrievals from ABI can be combined with those from other advanced instruments operating at the same time. These instruments will include Visible/Infrared Imager and Radiometer Suite (VIIRS; Hutchison et al., 2005), and hopefully the Earth Radiation Budget Sensor or a similar broadband instrument. The similarity of the ABI and VIIRS spectral channels and that of the aerosol algorithms proposed for both offer an excellent opportunity for synergy.

Acknowledgements

This work was supported in part by the NOAA/NESDIS GOES-R Risk Reduction and Algorithm Working Group Programs and by the NOAA/NESDIS GOES Product Systems Development and Implementation (G-PSDI) program. Thanks are due to Paul Menzel, former NESDIS/ORA Chief Scientist and to Don Gray, G-PSDI Program Manager for their encouragement and support, and to two anonymous reviewers for their thoughtful comments on the manuscript. Although this work was internally reviewed, the views, opinions, and findings contained in it are those of the authors and should not be construed as an official NOAA or US Government position, policy, or decision.

References

Augustine, J.A., DeLuisi, J.J., Long, C.N. SURFRAD – A national surface radiation budget network for atmospheric research. Bull. Amer. Meteor. Soc. 81, 2341–2357, 2000.

Charlock, T.P., Rose, F.G., Rutan, D.A., Kratz, D.P., Jin, Z., Coleman, L.H., Fu, Q. Relationship of Tropical Circulation and Energetics using Retrieved Surface and Atmospheric Radiation Budget for January–August 1998, in: Proceedings of 11th Conference on Atmospheric Radiation (AMS), 3–7 June 2002 in Ogden, Utah, pp. 28–31, 2002.

Christopher, S.A., Zhang, J., Holben, B.N., Yang, S.-K. GOES-8 and NOAA-14 AVHRR retrieval of smoke aerosol optical thickness during SCAR-B. Int. J. Remote Sens. 23, 4931–4944, 2002.

Cox, C., Munk, W. Statistics of the sea surface derived from sun glitter. J. Mar. Res. 13, 198–208, 1954.

Fraser, R.S., Kaufman, Y.J., Mahoney, R.L. Satellite measurements of aerosol mass and transport. Atmos. Environ. 18, 2577–2584, 1984.

Futyan, J.M., Russell, J.E., Harries, J.E. Determining cloud forcing by cloud type from geostationary satellite data. Geophys. Res. Lett. 32, L08807, doi:10.1029/2004GL022275, 2005.

Gautier, C., Diak, G.R., Masse, S. A simple physical model to estimate incident solar radiation at the surface from GOES satellite data. J. Appl. Meteor. 19, 1007–1012, 1980.

Harries, J.E., Russell, J.E., Hanafin, J.A., et al. The Geostationary Earth Radiation Budget Project. Bull. Amer. Meteor. Soc. 86, 945–960, doi:10.1175/BAMS-86-7-945, 2005.

Harrison, E.F., Minnis, P. Influence of clouds on the earth's radiation budget determined from GOES data, in: Fifth Conference on

Atmospheric Radiation, Baltimore, MD, October 31–November 4, 1983, Preprints (A85-32851 14-42), Boston, MA, American Meteorological Society, pp. 421–424, 1983.

Holben, B.N., Eck, T.F., Slutsker, I., Tanré, D., Buis, J.P., Setzer, A.W., Vermote, E.F., Reagan, J.A., Kaufman, Y.J., Nakajima, T., Lavenu, F., Jankowiak, I., Smirnov, A. AERONET – a federated instrument network and data archive for aerosol characterization. Remote Sens. Environ. 66, 1–16, 1998.

Hutchison, K.D., Roskovensky, J.K., Jackson, J.M., Heidinger, A.K., Kopp, T.J., Pavolonis, M.J., Frey, R. Automated cloud detection and classification of data collected by the visible infrared imager radiometer suite (VIIRS). Int. J. Remote Sens. 26, 4681–4706, 2005.

Ignatov, A. Spurious signals in TRMM/VIRS reflectance channels and their effect on aerosol retrievals. J. Atmos. Ocean. Technol. 20, 1120–1137, 2003.

Ignatov, A., Cao, C., Sullivan, J., Levin, R., Wu, X., Galvin, R. The usefulness of in-flight measurements of space count to improve calibration of the AVHRR solar reflectance bands. J. Atmos. Ocean. Technol. 22, 180–200, 2005.

Kahn, R., Banerjee, P., McDonald, D. The sensitivity of multi-angle imaging to natural mixtures of aerosols over ocean. J. Geophys. Res. 106, 18219–18238, 2001.

Kaufman, Y.J., Tanré, D., Remer, L.A., Vermote, E.F., Chu, A., Holben, B.N. Operational remote sensing of tropospheric aerosol over land from EOS moderate resolution imaging spectroradiometer. J. Geophys. Res. 102 (D14), 17051–17067, 1997.

Kaufman, Y.J., Gobron, N., Pinty, B., Widlowski, J.-L., Verstraete, M.M. Relationship between surface reflectance in the visible and mid-IR used in MODIS aerosol algorithm-theory. Geophys. Res. Lett. 29 (23), 2116, doi:10.1029/2001GL014492, 2002.

King, M.D., Kaufman, Y.J., Menzel, W.P., Tanré, D. Remote sensing of cloud, aerosol and water vapor properties from the Moderate Resolution Imaging Spectrometer (MODIS). IEEE Trans. Geosci. Remote Sens. 30, 2–27, 1992.

Knapp, K.R. Quantification of aerosol signal in GOES 8 visible imagery over the United States. J. Geophys. Res. 107 (D20), 4426, doi:10.1029/2001JD002001, 2002.

Knapp, K.R., Vonder Haar, T.H. Calibration of the eighth Geostationary Operational Environmental Satellite (GOES-8) imager visible sensor. J. Atmos. Ocean. Technol. 17, 1639–1644, 2000.

Knapp, K.R., Vonder Haar, T.H., Kaufman, Y.J. Aerosol optical depth retrieval from GOES-8: Uncertainty study and retrieval validation over South America. J. Geophys. Res. 107 (D7), doi:10.1029/2001JD000505, 2002.

Knapp, K.R., Frouin, R., Kondragunta, S., Prados, A. Toward aerosol optical depth retrievals over land from GOES visible radiances: determining surface reflectance. Int. J. Remote Sens. 26, 4097–4116, 2005.

Laszlo, I., Pinker, R.T. Shortwave radiation budget of the Earth: absorption and cloud radiative effects, Időjárás. Quarterly Journal of the Hungarian Meteorological Service. 106, 189–205, 2002.

Laszlo, I., Jacobowitz, H., Gruber, A. The relative merits of narrowband channels for estimating broadband albedos. J. Atmos. Ocean. Technol. 5, 757–773, 1988.

Loeb, N.G., Kato, S., Loukachine, K., Manalo-Smith, N. Angular distribution models for top-of-atmosphere radiative flux estimation from the Clouds and the Earth's Radiant Energy System instrument on the Terra Satellite. Part I: Methodology. J. Atmos. Ocean. Technol. 22, 338–351, 2005.

Pavolonis, M.J., Heidinger, A.K., Uttal, T. Daytime global cloud typing from AVHRR and VIIRS: Algorithm description, validation, and comparisons. J. Appl. Meteor. 44, 804–826, 2005.

Pinker, R.T., Laszlo, I. Modeling surface solar irradiance for satellite applications on a global scale. J. Appl. Meteor. 31, 194–211, 1992.

Pinker, R.T., Laszlo, I., Tarpley, J.D., Mitchell, K. Geostationary satellite products for surface energy balance models. Adv. Space Res. 30, 2427–2432, 2002.

Pinker, R.T., Tarpley, J.D., Laszlo, I., et al. Surface radiation budgets in support of the GEWEX Continental-Scale International Project (GCIP) and the GEWEX Americas Prediction Project (GAPP), including the North American Land Data Assimilation System (NLDAS) project. J. Geophys. Res. 108 (D22), 8844, doi:10.1029/2002JD003301, 2003.

Pinty, B., Roveda, F., Verstraete, M.M., Gobron, N., Govaerts, Y., Martonchik, J.V., Diner, D.J., Kahn, R.A. Surface albedo retrieval from Meteosat, 1. Theory. J. Geophys. Res. 105 (D14), 18,099–18,112, 2000a.

Pinty, B., Roveda, F., Verstraete, M.M., Gobron, N., Govaerts, Y., Martonchik, J.V., Diner, D.J., Kahn, R.A. Surface albedo retrieval from Meteosat, 2. Applications. J. Geophys. Res. 105 (D14), 18,113–18,134, 2000b.

Remer, L.A., Kaufman, Y.J., Tanré, D., Mattoo, S., Chu, D.A., Martins, J.V., Li, R.-R., Ichoku, C., Levy, R.C., Kleidman, R.G., Eck, T.F., Vermote, E., Holben, B.N. The MODIS aerosol algorithm, products, and validation. J. Atmos. Sci. 62 (4), 947–973, 2005.

Rutan, D.A., Charlock, T.P. Validation of CERES/SARB data product using ARM surface flux observations, in: 14th ARM Science Team Meeting Proceedings, Albuquerque, New Mexico, March 22–26, 2004, (http://www.arm.gov/publications/proceedings/conf14/extended_abs/rutan-da.pdf), 2004.

Schiffer, R.A., Rossow, W.B. The International Satellite Cloud Climatology Project (ISCCP): the first project of the World Climate Research Programme. Bull. Amer. Meteor. Soc. 64, 779–984, 1983.

Schmit, T.J., Gunshor, M.M., Menzel, W.P., Gurka, J.J., Li, J., Bachmeier, A.S. Introducing the next generation advanced baseline imager on GOES-R. Bull. Amer. Meteor. Soc. 86, 1079–1096, 2005.

Tanré, D., Kaufman, Y.J., Herman, M., Mattoo, S. Remote sensing of aerosol properties over oceans using the MODIS/EOS spectral radiances. J. Geophys. Res. 102 (D14), 16971–16988, 1997.

Tarpley, J.D. Estimating incident solar radiation at the surface from geostationary satellite data. J. Appl. Meteor. 18, 1172–1181, 1979.

Vermote, E.F., Tanré, D., Deuzé, J.L., Herman, M., Morcrette, J.-J. Second simulation of the satellite signal in the solar spectrum, 6S: an overview. IEEE Trans. Geosci. Remote Sens. 35, 675–686, 1997.

Wielicki, B., Barkstrom, R., Harrison, E.F., Lee III, R.B., Smith, G.L., Cooper, J.E. Clouds and the Earth's Radiant Energy System (CERES): an earth observing system experiment. Bull. Amer. Meteor. Soc. 77, 853–868, 1996.

Zhang, J., Christopher, S.A., Holben, B.N. Intercomparison of smoke aerosol optical thickness derived from GOES-8 imager and ground-based sun photometers. J. Geophys. Res. 106, 7387–7397, 2001.